Available online at www.sciencedirect.com
SCIENCE DIRECT
ELSEVIER
Genomics 87 (2006) 243–253
GENOMICS
www.elsevier.com/locate/ygeno

The novel centrosomal associated protein CEP55 is present in the spindle midzone and the midbody ☆

Isabel Martinez-Garay [a,1], Amin Rustom [b,1], Hans-Hermann Gerdes [b,c], Kerstin Kutsche [a,*]

[a] *Institut für Humangenetik, Universitätsklinikum Hamburg-Eppendorf, Butenfeld 42, D-22529 Hamburg, Germany*
[b] *Interdisciplinary Center of Neuroscience (IZN), Institute of Neurobiology, University of Heidelberg, INF 364, 69120 Heidelberg, Germany*
[c] *Department of Biomedicine, Section of Biochemistry and Molecular Biology, University of Bergen, 5009 Bergen, Norway*

Received 19 July 2005; accepted 16 November 2005

Abstract

Centrosomes are the major microtubule nucleating center in the cell; they also contribute to spindle pole organization and play a role in cell cycle progression as well as completing cytokinesis. Here we describe the molecular characterization of a novel human gene, *CEP55*, located in 10q23.33 that is expressed in multiple tissues and various cancer cell lines. Sequence analysis of the cDNA predicted a protein of 464 amino acids with several putative coiled-coil domains that are responsible for protein–protein interactions. Indeed, we found homodimerization of CEP55 by coimmunoprecipitation. Subcellular localization analysis revealed that endogenous CEP55 as well as an EGFP–CEP55 fusion protein is present at the centrosome throughout mitosis, whereas it also appears at the cleavage furrow in late anaphase and in the midbody in cytokinesis. Neither nocodazole nor taxol interfered with centrosome association of endogenous CEP55, suggesting that it directly interacts with centrosome components rather than with microtubules. In microtubule regrowth assays, overexpression of CEP55 did not enhance or inhibit microtubule nucleation. Together, these data suggest a possible involvement of CEP55 in centrosome-dependent cellular functions, such as centrosome duplication and/or cell cycle progression, or in the regulation of cytokinesis.

Keywords: CEP55; Centrosome; Spindle midzone; Midbody; Mitosis; Cytokinesis; Cell cycle; EGFP; γ-Tubulin; Coiled-coil

Introduction

The centrosome has been regarded as the special organ of cell division since its discovery in 1875. In most vertebrate cells, centrosomes are composed of two main substructures, the centrioles and the pericentriolar material (PCM) [1]. Centrioles are located in the centrosome core and comprise a pair of barrel-shaped arrays, each composed of nine sets of triplet microtubules that are arranged as a pinwheel. Centrioles can be distinguished by the presence or absence of additional appendages and are described as mother and daughter centriole. The pericentriolar material surrounds both centrioles and is the main site of microtubule nucleation. Although a particular molecular organization has not yet been described for the PCM, it is a dynamic matrix of fibers and protein aggregates [1]. Different classes of centrosomal proteins are known. The first class comprises proteins that are responsible for maintaining the structure of the centrosome and they serve as a scaffold for the assembly of other proteins. Proteins that function in microtubule nucleation belong to the second group. So-called anchoring elements, constituting the third group, form the interface between microtubule nucleator proteins and regulatory molecules. These latter proteins represent the fourth class, including kinases, phosphatases, and signaling molecules [2]. The majority of proteins associated with the centrosome are structural proteins that are enriched in coiled-coil domains as their predominant structural feature [3,4]. Coiled-coil domains are the most commonly known oligomerization motifs in proteins and comprise two to five right-handed amphipathic α-helices that coil around one another to form a left-handed supercoil [5]. In general, two groups of coiled-coil proteins can

☆ Sequence data from this article have been deposited with the EMBL/GenBank Data Libraries under Accession No. AY788918 (*CEP55*).

* Corresponding author. Fax: +49 40 42803 5138.
E-mail address: kkutsche@uke.uni-hamburg.de (K. Kutsche).

[1] Both authors contributed equally to this work.

0888-7543/$ - see front matter © 2005 Elsevier Inc. All rights reserved.
doi:10.1016/j.ygeno.2005.11.006

be distinguished. Short coiled-coil motifs are often found as dimerization domains and preferentially form homo- or heterodimers and, thus, mediate specific protein–protein interactions [6]. Long coiled-coil domains, which encompass several hundred amino acids, usually form "rod-like" tertiary structures. These latter proteins are involved in diverse cellular functions [6].

The centrosome needs to be duplicated once every cell cycle. In a G1-phase cell, a single centrosome that is duplicated during the S phase of the cell cycle is present. At the G2–M transition, centrosome maturation occurs. During mitosis, centrosomes separate from each other and form the two spindle poles. However, recent data suggest that centrosomes are not essential for spindle assembly in mammalian cells [7,8], although when present, they have a dominant role in the formation of the spindle poles [9]. Finally, in cytokinesis, each daughter cell inherits one centrosome. Remarkably, centrosomal abnormalities are frequently found in many common cancers [10–12].

The centrosome was found to be required for cell cycle progression through G1–S phase and plays a role in regulating exit from cytokinesis [7,8,13]. These data indicate a direct link between the centrosome and checkpoint control mechanisms by either activating final steps of cytokinesis or releasing the cells from a checkpoint that monitors the completion of mitosis [14,15].

Here we describe the characterization of a novel human gene, *CEP55* (*centrosomal protein, 55 kDA*), located in 10q23.33 that encodes a protein capable of homodimerization. During mitosis, subcellular localization of the endogenous protein showed that CEP55 is associated with the centrosome in all stages of mitosis. In anaphase, CEP55 also appears in the midzone and during cytokinesis it concentrates in the midbody. Remarkably, *CEP55* was found to be located in the 10q24 breakpoint region of an X;10 translocation in a patient with multiple clinical signs and symptoms.

Results

cDNA sequence and expression pattern of CEP55

Molecular characterization of an X;10 translocation in a patient with a complex phenotype [16] revealed 26 PAC clones overlapping the breakpoint on 10q24 by fluorescence *in situ* hybridization (data not shown). The identification of such a large number of breakpoint-spanning clones containing no regions in common suggested the presence of a complex rearrangement in the patient, i.e., a duplication in addition to the translocation. To characterize novel genes located in 10q24, we performed exon-trapping experiments with one overlapping PAC clone, C07950, and identified three putative exons showing sequence identity to five EST clones, 305497, 242048, 199614, 504308, and 930287. We sequenced the EST inserts and assembled a cDNA sequence that contained a putative open reading frame (ORF), but no ATG start codon. BLASTN analysis against genomic sequences revealed that the gene is present on BAC clone RP11-30E16 (GenBank Accession No. AL356214). This genomic sequence was used for RUMMAGE analysis that led to the prediction of further 5′ cDNA sequence harboring an ATG start codon. Subsequently, we carried out RT-PCR analysis with a forward primer located in the predicted cDNA sequence and a reverse primer in the assembled cDNA sequence and obtained an amplicon that was cloned and sequenced. In total, we generated a cDNA sequence of 2634 bp containing a possible start codon and an ORF of 1395 bp that encodes a putative protein of 464 amino acids. We found a homologous human cDNA sequence in the database with GenBank Accession No. AK001402, named *C10orf3*. In the 2634-bp cDNA sequence, no stop codon upstream of the putative ATG codon is present, suggesting that the ORF is still not complete and extends in the 5′ direction. BLASTP analysis of the amino acid sequences of human and mouse C10orf3 revealed that the human open reading frame shows 75% identity and 86% similarity to the mouse protein (data not shown). The homology between both amino acid sequences starts with the first methionine. Moreover, a stop codon is located 15 bp upstream of the start codon in the murine cDNA sequence, suggesting that the identified ATG triplet in the human cDNA represents the proper start codon. BLASTN analysis using the human cDNA sequence against genomic sequences showed that the gene is composed of nine exons spanning a genomic region of 32,458 bp. The start codon lies in exon 2 and the stop codon is located in exon 9. Further characterization of the protein encoded by this gene (see below) resulted in renaming it *CEP55*, centrosomal protein, 55 kDA.

We used various computer analysis software programs, including PROSITE, SMART, PFAM, FALTA, and PSORT, to analyze the deduced amino acid sequence of the human CEP55 ORF. No significant homologies to other proteins or domains were found. However, a database search at the NCBI BLAST Network Service using the Conserved Domain (CD) database revealed partial homology to chromosome segregation ATPases that play a role in cell division and chromosome partitioning.

We analyzed expression of *CEP55* by probing a multiple adult human tissue Northern blot. A transcript of ~2800 nt was detected that corresponds well to the cDNA sequence of 2634 bp, suggesting that we obtained the full-length cDNA. We observed strong expression of *CEP55* in thymus and weak expression in colon, small intestine, and placenta (Fig. 1A). To confirm the expression pattern, we probed a commercially available RNA array from multiple human tissues and observed a strong signal in testis and intermediate signals in adult and fetal thymus as well as in various cancer cell lines. Low-level expression was found in different parts of the digestive tract, bone marrow, lymph nodes, placenta, fetal heart, and fetal spleen (Fig. 1B). In summary, *CEP55* expression is clearly detectable in highly proliferating tissues, whereas in tissues with low proliferative activity, such as brain, almost no signals could be observed. However, expression of *CEP55* was present in all tissues of the multiple-tissue RNA array after a long exposition time (data not shown).

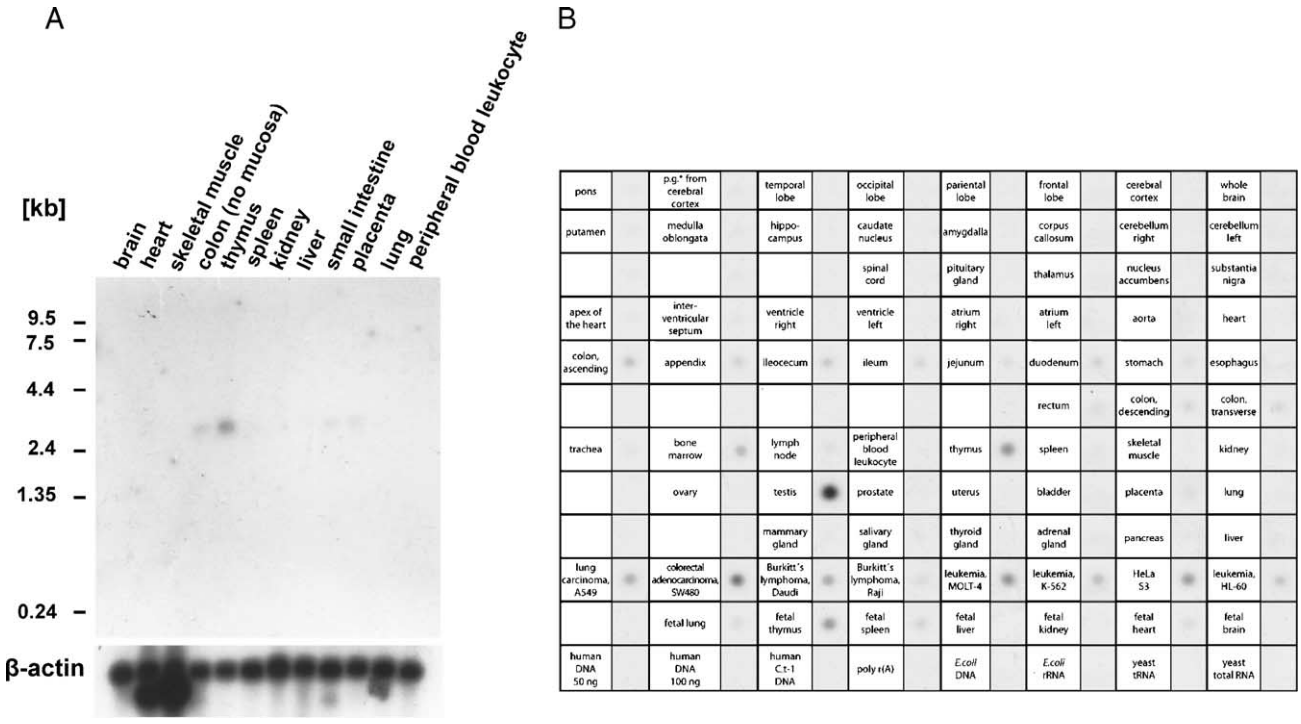

Fig. 1. The *CEP55* transcript is highly expressed in testis, thymus, bone marrow, and various cancer cell lines. (A) Hybridization of part of the coding region of *CEP55* to an adult human multiple tissue Northern blot containing total RNA. A single transcript of ~2800 nt was detectable in colon, thymus, small intestine, and placenta, with strongest expression in thymus. The same blot was reprobed with a β-actin probe. (B) Hybridization of the same probe to a commercially available RNA (MTE) array. Hybridization signals are shown that are represented by dots of differing shades of gray.

CEP55 was predicted to contain numerous coiled-coil regions and shows homophilic binding

To analyze possible secondary structures of CEP55, we used different programs predicting coiled-coil regions (COILS, PAIRCOIL, and MULTICOIL). At least six putative coiled-coil motifs are scattered along the entire amino acid sequence of CEP55 (Fig. 2A), offering CEP55 the potential to homo- or heterodimerize and form higher-order oligomers. We coexpressed full-length FLAG- and HA-tagged CEP55 in CHO-K1 cells and performed coimmunoprecipitation experiments with anti-FLAG antibody. As shown in Fig. 2B, HA-tagged CEP55 was detected in precipitates of cell lysates transfected with FLAG-CEP55 cDNA (Fig. 2B, top, lane 2), but not in those obtained after transfection with empty FLAG-vector (Fig. 2B, top, lane 1). These data suggest that CEP55 is able to form homodimers in CHO-K1 cells *in vivo*.

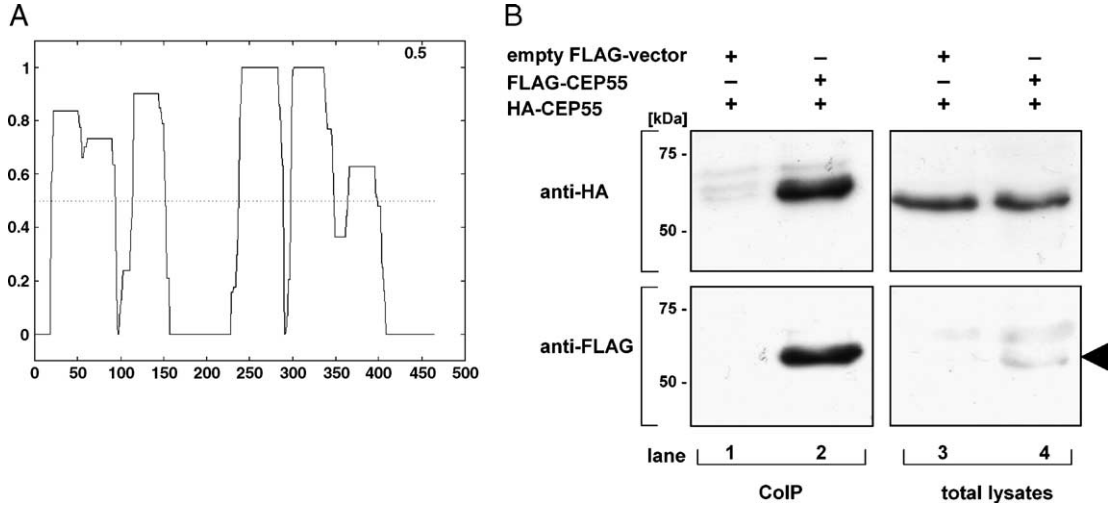

Fig. 2. CEP55 contains numerous coiled-coil motifs and shows homophilic binding. (A) Schematic representation of the coiled-coil prediction of CEP55 obtained by the PAIRCOIL program (http://paircoil.lcs.mit.edu/cgi-bin/paircoil). (B) Identification of CEP55 homophilic binding by coimmunoprecipitation experiments. CHO-K1 cells were transfected with both FLAG- and HA-tagged constructs of CEP55. HA-tagged CEP55 was detected after coimmunoprecipitation with anti-FLAG antibody. Expression of FLAG-tagged proteins in lysates (indicated by an arrowhead in the bottom, lane 4) and precipitates (bottom, lane 2) was confirmed by immunoblot.

Centrosomal localization of endogenous and EGFP-tagged CEP55 during mitosis

The specificity of polyclonal antibodies raised against the first 250 amino acids of CEP55 was demonstrated by Western blot analysis of cell lysates prepared from CHO-K1 cells ectopically expressing HA- or EGFP-tagged CEP55 protein (Fig. 3). It is of note that endogenous CEP55 protein was not detected (Fig. 3, left lane). This suggests that the CEP55 protein expression level is low, which is in line with the expression data obtained by Northern blot analysis (Fig. 1).

To obtain first insights into the biological function of CEP55, we determined the subcellular localization of the endogenous protein. Therefore, CHO-K1 cells were coimmunostained with antibodies against CEP55 and α-tubulin and analyzed by fluorescence microscopy. In interphase cells, CEP55 signals could be detected as one or two closely spaced dots, which are usually located close to the nuclear envelope (Figs. 4A–4C, and data not shown). These intense dots are present in the area of the microtubule organization center (MTOC), suggesting that they represent centrosomes. Additionally, numerous small vesicular structures were detected in the cytoplasm (indicated by arrowheads in Fig. 4A). In prophase and metaphase, prominent CEP55 signals were detectable at the spindle poles (Figs. 4D–4I). Remarkably, staining of CEP55 was found at the cleavage furrow as well as at the spindle poles during late anaphase (Figs. 4J–4L). In addition, we observed an elevated green fluorescence, indicative of the presence of CEP55, in the cytoplasm during this stage of mitosis (Figs. 4J and 4L). Finally, a prominent staining was detected in the central region of the cytoplasmic bridge, the midbody, although a weak staining still remained at the centrosomes in telophase (Figs. 4M–4O). Together these results show that CEP55 is associated with the centrosome throughout mitosis and concentrates in the midbody in cytokinesis. It is important to note that we observed no such staining with the pre-immune serum (data not shown).

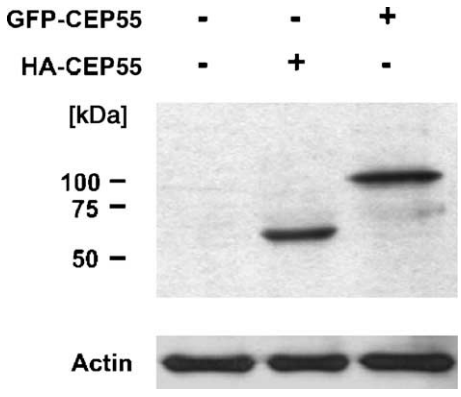

Fig. 3. Specific detection of ectopically expressed CEP55 by anti-CEP55 antibodies. CHO-K1 cells, either nontransfected or transfected with HA- or EGFP-tagged CEP55, were lysed, protein lysates were separated by SDS–PAGE, and immunoblot was performed with anti-CEP55 antibodies. Expression of HA- or EGFP-tagged CEP55 protein was specifically detected by the anti-CEP55 antibodies (top, middle and right lanes), whereas the endogenous CEP55 protein could not be detected (top, left lane). As a control, the expression of actin was confirmed in all cell lysates (bottom).

Next, we wanted to analyze the cellular distribution of CEP55 in more detail and generated CHO-K1 cells stably expressing an N-terminal tagged EGFP–CEP55 fusion protein. We synchronized the cells to study the cellular distribution of the fusion protein compared to the endogenous protein. Indeed, the EGFP–CEP55 protein showed a very similar subcellular localization as the endogenous CEP55 during mitosis (Fig. 5). Staining of cells with anti-γ-tubulin antibodies revealed colocalization of EGFP–CEP55 with γ-tubulin in prophase, indicating that CEP55 shows a centrosomal localization (Fig. 5C). Together, the cellular distribution of EGFP–CEP55 that matches that of the endogenous protein makes it a suitable tool to analyze the dynamics of CEP55 redistribution during mitosis.

EGFP–CEP55 resides at the centrosome in all stages of mitosis but also appears in the spindle midzone during anaphase and in the midbody in postmitotic stages

We performed live-cell videomicroscopy on synchronized CHO-K1 cells stably expressing EGFP–CEP55. In prophase, two prominent diffuse accumulations of green fluorescence at the centrosomes could be observed (Figs. 6A–6C, and Supplementary Data). Some very faint vesicular structures moving inside the cell were also detected (video available as Supplementary Data). In metaphase, a diffuse cytoplasmic labeling was apparent in addition to the signals at the centrosomes (Figs. 6D and 6E). With the beginning of anaphase, a weak signal at the central region of the spindle became visible (Fig. 6F). Interestingly, this staining was remarkably granular/vesicular. However, no transport of vesicular structures to the central region could be detected. The fluorescence signal at the central region increased until telophase onset (Fig. 6G). In parallel, a slight reduction of the cytoplasmic EGFP–CEP55-signal could be observed. When the contractile ring started to cord up, the signal at the central region became more and more concentrated (Figs. 6H–6L), resulting in a brightly fluorescent midbody during cytokinesis (Fig. 6M). The signal at the centrosomes remained mainly unchanged during the whole process. Thus, it appears unlikely that CEP55 was redistributed from the centrosome to the spindle midzone. Instead, our data suggest that CEP55 might be recruited from a cytoplasmic pool to the spindle midzone.

Centrosome association of CEP55 is independent of microtubules and CEP55 overexpression does not seem to have any effect on microtubule nucleation

CHO-K1 cells were cultivated in the presence of nocodazole and taxol, respectively. Nocodazole results in depolymerization of the cytoplasmic microtubule network, whereas taxol treatment has a stabilizing effect on microtubules, leading to long microtubule bundles and loss of centrosome-nucleated microtubules [17]. If CEP55 binds to microtubules, its

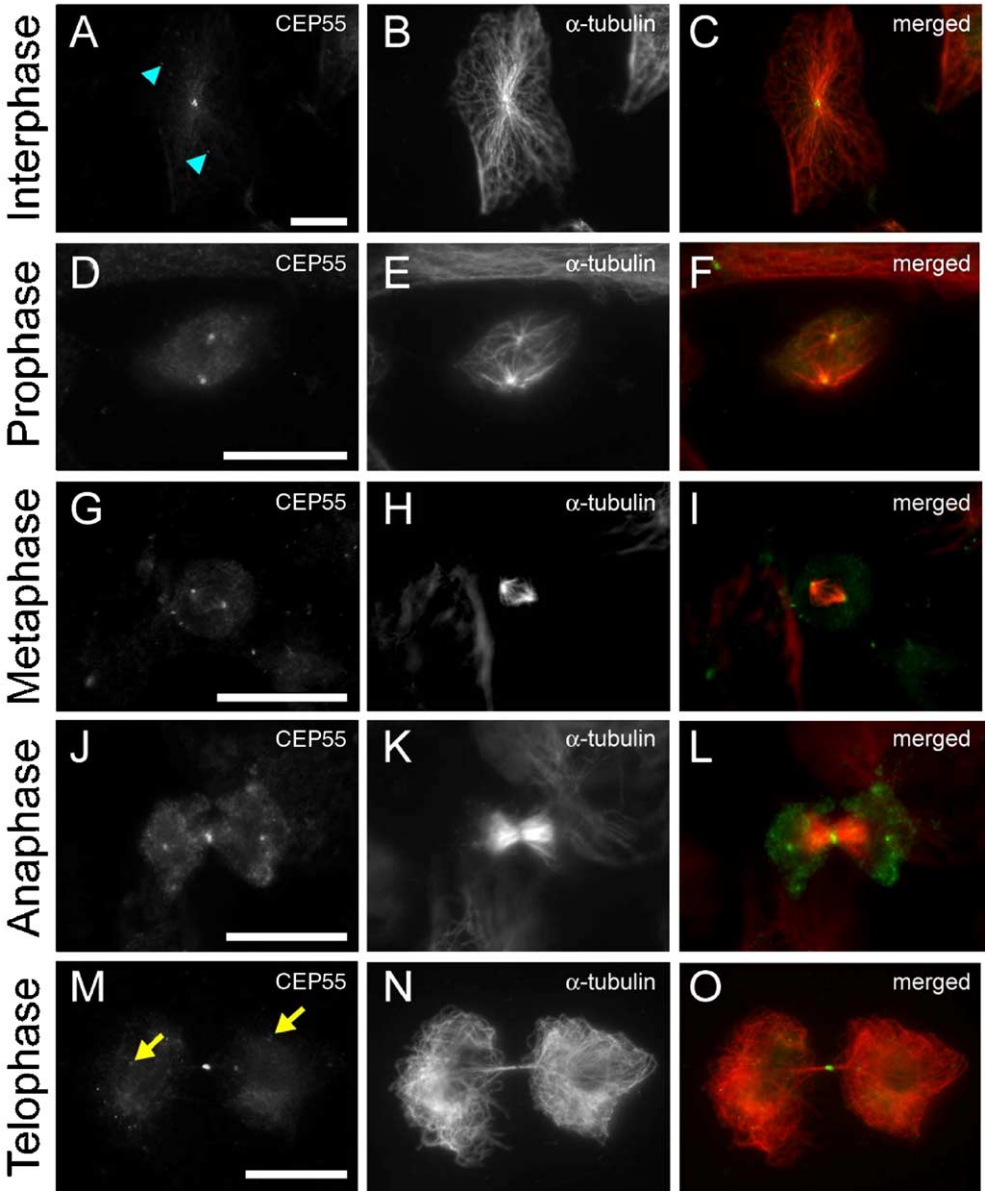

Fig. 4. Endogenous CEP55 is present at the centrosome in all stages of mitosis, appears at the cleavage furrow in late anaphase, and concentrates at the center of the midbody in cytokinesis. CHO-K1 cells were costained with anti-CEP55 and anti-α-tubulin antibodies. In interphase, CEP55 was present in one dot in the cell (A) and is located in the MTOC area (C). Light blue arrowheads point to the localization of CEP55 in small vesicular structures in the cell (A). In prophase and metaphase cells, CEP55 appeared at the spindle poles (D, F, G, and I). CEP55 was present at the cleavage furrow, at the spindle poles, and in the cytoplasm in late anaphase (J and L), and concentrated in the midbody during cytokinesis (M and O). Nonetheless, CEP55 is still faintly visible at the centrosomes (yellow arrows in M). The scale bars represent 10 μm.

subcellular distribution should change in concert with the subcellular distribution of α- or γ-tubulin. In CHO-K1 cells incubated with taxol and stained with anti-α- and anti-γ-tubulin antibodies as well as anti-CEP55 antibodies, the microtubules appeared as dense bundles that were detached from the centrosomes in the majority of cells (Fig. 7D). In these cells, CEP55 staining was still restricted to punctated signals (Fig. 7E) and colocalization of CEP55 with γ-tubulin was observed in the presence of taxol-induced asters (Fig. 7F). In cells treated with nocodazole and costained with the anti-α- and anti-γ-tubulin antibodies, microtubules were completely absent (Fig. 7G). However, endogenous CEP55 was still present at the centrosome (Fig. 7H) as shown by colocalization with γ-tubulin (Fig. 7I).

To analyze whether overexpression of CEP55 has any effect on microtubule nucleation, we performed a microtubule regrowth assay with nontransfected cells and cells that transiently expressed EGFP–CEP55. After microtubules were depolymerized, microtubule regrowth was induced and cells were fixed, costained with anti- γ- and anti-α-tubulin antibodies, and subsequently analyzed by immunofluorescence. EGFP–CEP55-expressing cells (Fig. 8D) showed one center of microtubule nucleation with many long and thin microtubules that arose from the centrosome (Fig. 8F). Under these conditions, no additional

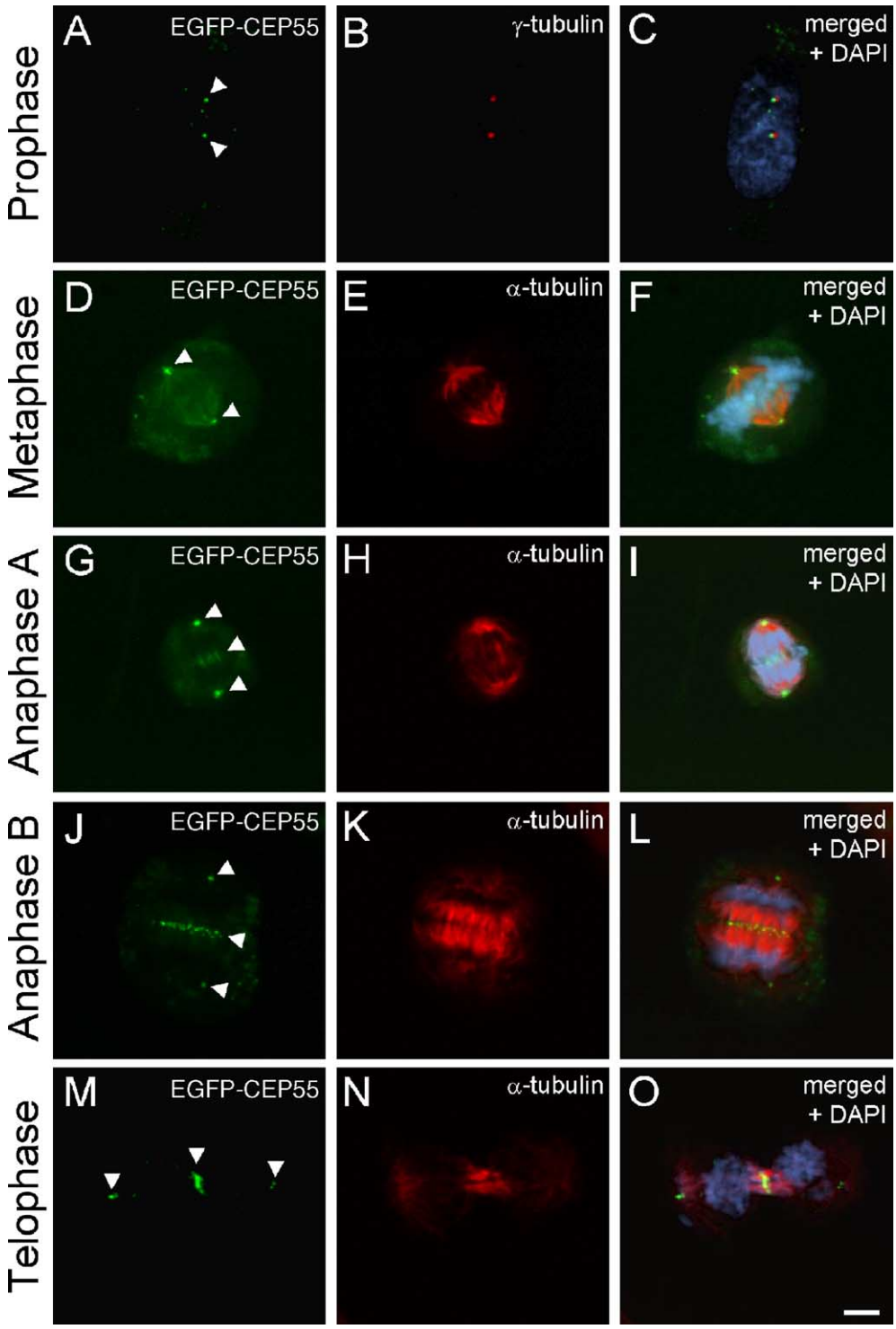

Fig. 5. EGFP–CEP55 shows a subcellular localization comparable to the endogenous protein. CHO-K1 cells stably expressing EGFP–CEP55 were incubated with thymidine. Subsequently, cells were washed and incubated at 37°C for 5 h. A second incubation step for 5 h with nocodazole was performed to arrest the cells at prometaphase. To obtain cells during different mitotic stages, nocodazole was washed out and preextraction followed by methanol fixation was performed at multiple time points. Cells in prophase were stained with an anti-γ-tubulin antibody (B), whereas cells in all other mitotic stages were stained with an anti-α-tubulin antibody (E, H, K, N). DAPI was used to visualize DNA (C, F, I, L, O). Arrowheads point to the localization of the EGFP–CEP55 fusion protein. In prophase, EGFP–CEP55 was present in two dots in the cell (A) and colocalized with γ-tubulin at the centrosomes (C). In metaphase cells, EGFP–CEP55 appeared at the centrosome (D, F). During anaphase A, EGFP–CEP55 remained at the centrosome; however, it also started to accumulate in the spindle midzone (G, I). This localization became more apparent in anaphase B (J, L). During cytokinesis, the EGFP–CEP55 protein was visible in the midbody (M, O). Nonetheless, a centrosomal localization was still present in anaphase B and cytokinesis (L, O). The scale bar represents 10 μm.

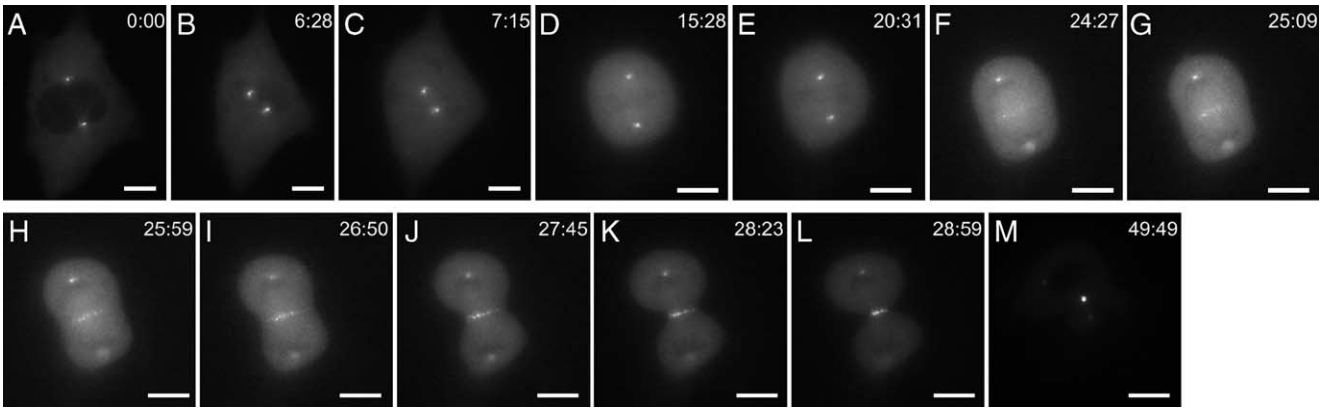

Fig. 6. Dynamics of CEP55 redistribution during mitosis. CHO-K1 cells stably expressing EGFP–CEP55 were synchronized as described in the legend to Fig. 5. After nocodazole was washed out, cells were directly analyzed using live-cell fluorescence microscopy. Selected frames of a videosequence covering 52 min are depicted, showing an EGFP–CEP55-positive cell passing through mitosis. Prometaphase (A–C); metaphase (D and E); anaphase (F and G); telophase (H–K); cytokinesis (L and M). Note the fluorescence signals at the centrosomes, the increasing, granular/vesicular signal at the central region of the spindle (F–J), and the concentrated signal at the midbody (M). The corresponding videosequence is available as supplementary material. The scale bars represent 10 μm.

asters could be seen compared to untransfected cells (Figs. 8A and 8C). Thus, overexpression of CEP55 neither enhances nor perturbs the assembly of microtubules.

Discussion

During molecular characterization of an X;10 translocation in a patient with various clinical signs and symptoms, we ended with the finding of a putative complex rearrangement in the 10q24 breakpoint region that significantly hampered determination of the sequences flanking the X chromosomal and the chromosome 10 breakpoints. However, we analyzed the X chromosome breakpoint in detail and identified the *FAM9* gene family present in Xp22.3 [16].

In an attempt to find novel genes located in the 10q24 breakpoint region, we characterized a 2634-bp cDNA that is expressed in thymus, colon, small intestine, placenta, different parts of the digestive tract, bone marrow, lymph nodes, fetal heart, and fetal spleen as well as in various cancer cell lines. This gene was designated *CEP55* (*centrosomal protein, 55 kDA*) and spans nine exons on genomic DNA. We used numerous computer programs for the identification of putative protein motifs and observed multiple short coiled-coil domains spanning almost continuously the length of the amino acid sequence. These coiled-coil motifs are frequently found to be responsible for homo- and heterodimerization and, thus, mediate protein–protein interactions [6]. Indeed, we showed homodimerization of CEP55, suggesting that higher oligomer structures can be formed. Proteins containing coiled-coil motifs are highly enriched in the pericentriolar matrix surrounding

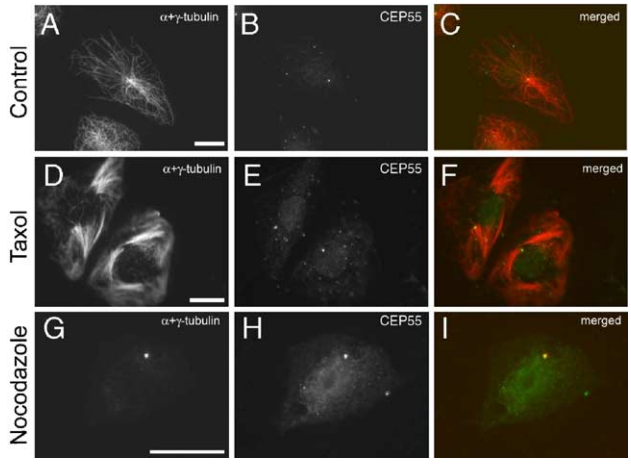

Fig. 7. CEP55 remains associated with the centrosome in cells treated with either nocodazole or taxol. CHO-K1 cells were incubated with taxol to stabilize microtubuli and detach them from the centrosome. Cells were subsequently preextracted and fixed with methanol, and staining of untreated (A–C) or treated cells was performed with anti-α- and anti-γ-tubulin antibodies and anti-CEP55 antibodies. All cells were affected by the taxol treatment since microtubules appeared as dense bundles (D). CEP55 localization was restricted to various dots in the cell (E) and colocalization with γ-tubulin was observed (F). CHO-K1 cells were incubated with nocodazole to depolymerize microtubuli. Costaining of cells with anti-α- and anti-γ-tubulin antibodies as well as anti-CEP55 antibodies showed the complete absence of microtubuli in the cell (G). A CEP55 signal is still visible at the centrosome (H). When images were overlaid, the yellow signal generated indicated colocalization of CEP55 with γ-tubulin (I). The scale bars represent 10 μm.

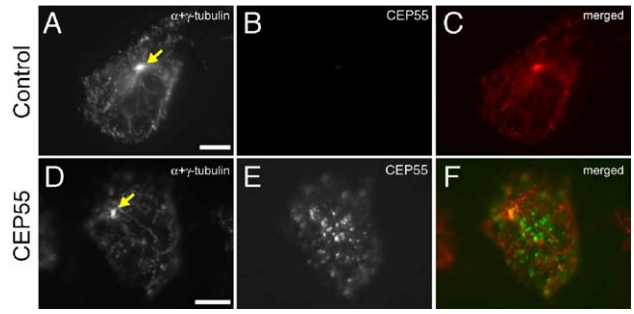

Fig. 8. Overexpression of CEP55 does not affect microtubule nucleation. For the microtubule regrowth assay, nontransfected and transiently expressing EGFP–CEP55 cells were treated with nocodazole, washed, and placed into fresh medium. Cells were costained with anti-α- and anti-γ-tubulin antibodies (A and D). Only one center of organized microtubules, the centrosome, is visible in nontransfected (A) and EGFP–CEP55-transfected cells (D) (yellow arrows). Colocalization of EGFP–CEP55 with γ-tubulin at the centrosome is shown by the yellow pseudo-color (F). The scale bars represent 10 μm.

centrosomes [4] and provide a scaffold for anchoring proteins that are required for, e.g., microtubule nucleation [14].

Subcellular localization studies of endogenous CEP55 as well as CEP55 fused to EGFP showed that it localized to the centrosome during all stages of mitosis as well as in paired cells that were still connected by postmitotic bridges (early G1 phase). These data suggest that CEP55 might be associated with the centrosome throughout the cell cycle, although we cannot yet exclude the possibility that CEP55 translocates to other sites within the cell during late G1 and/or S phase. The centrosomal association of CEP55 was found to be independent of microtubules, suggesting that CEP55 is a core component of the centrosome that might be recruited to the pericentriolar matrix by other yet to be defined proteins. Microtubule-independent centrosome association has been described for various proteins, such as CTCF [18], Nek2 [19], Cep135 [20], and γ-tubulin [21]. Moreover, the ectopic expression of CEP55 has no effect on microtubule regrowth, suggesting that CEP55 is most likely not involved in microtubule-dependent functions in the cell.

During anaphase, CEP55 is present at the centrosome and also appears in the spindle midzone. Finally, it becomes concentrated in the center of the midbody in cytokinesis. This specific cellular localization of CEP55, an α-helical protein, during mitosis raises the question of a possible involvement in centrosome function and/or regulation of cytokinesis as shown for other proteins. Recently, a novel coiled-coil protein, centriolin, of the maternal centriole that is present at the centrosome through all stages of the cell cycle has been described. However, during cytokinesis, centriolin initially appeared within the intercellular bridge and subsequently became concentrated in the midbody. Silencing of centriolin induces cytokinesis failure, indicating an important role for centriolin in the late stages of cytokinesis [22]. The protein tyrosine phosphatase PTP-BL localizes to the centrosomes in inter- and metaphase, is present in the midzone in anaphase, and accumulates in the midbody in cytokinesis. PTP-BL was also shown to be implicated in the regulation of cytokinesis [23]. Similarly, the presence of CEP55 in the spindle midzone and the midbody in addition to its centrosomal localization suggested a possible role of CEP55 in cytokinesis regulation.

A number of proteins that are not associated with the centrosome localize to the midzone of the mitotic spindle and the midbody, such as PRC1 and the citron-kinase [24,25]. Remarkably, PRC1 contains multiple coiled-coil motifs in its N-terminal region. PRC1 is a microtubule-associated protein that stabilizes the microtubule bundle of the midzone and is required to maintain the spindle midzone [25]. Similarly, the Rab6-binding kinesin protein Rab6-KIFL and the large GTPase dynamin accumulate in the midzone in anaphase and in the midbody in cytokinesis. For both proteins an important function in completion of cytokinesis has been suggested [26,27]. It is of interest to note that various midbody proteins have been shown to function in cell cycle regulation as well as in asymmetric cell division and chromosome segregation [28].

The localization of *CEP55* in a chromosomal region that is present in three copies in the genome of the t(X;10) patient led us to hypothesize that higher *CEP55* mRNA and protein levels might have contributed to the patient's phenotype. In this context, it is worth mentioning that mutations in three genes, namely, *BBS4*, *SPG4*, and *OFD1*, encoding proteins associated with the centrosome are known to be responsible for different human inherited disorders [29–31]. Thus, the recent discovery of defects in centrosome function or microtubule organization in human inherited diseases demonstrates that centrosome organization, centrosome-mediated microtubule events, and the possible involvement of the centrosome in the activation of checkpoints during cell cycle and cytokinesis [14] are important for proper function of various cell types and tissues [32]. Moreover, centrosomal aberrations have been noted to be involved in many common cancers, such as breast, colon, lung, and prostate [12]. Further studies are required to elucidate the precise cellular function of CEP55; however, given its centrosomal localization in all stages of mitosis and its presence in the spindle midzone and midbody, we assume that it might be implicated (directly or indirectly) in regulatory functions of the centrosome during the cell cycle and/or regulation of cytokinesis.

Materials and methods

DNA isolation of PAC clones and exon trapping

PAC clone RPCIP704C07950Q3 (C07950) was provided by the RZPD Deutsches Ressourcenzentrum für Genomforschung GmbH, Berlin, Germany. PAC DNA was prepared using a plasmid midiprep kit (Qiagen). PAC clone C07950 was digested with *Bam*HI, *Bgl*II, *Pst*I, and *Sac*I, respectively, and the resulting pools of fragments were cloned into pSPL3. Exon trapping was performed by the Exon Trapping System (Life Technologies/Invitrogen) following the manufacturer's instructions.

EST clones

EST clones 305497, 242048, 199614, 504308, and 930287 (GenBank Accession Nos. W39078, H94225, R96554, AA131908, and AA502823) were provided by the RZPD Deutsches Ressourcenzentrum für Genomforschung GmbH, Berlin, Germany. DNA inserts were sequenced using T7 and T3 primers and by primer walking (primer sequences are available from the authors on request).

RT-PCR

For RT-PCR, human testis poly(A) mRNA was used (BD Biosciences Clontech). First-strand cDNAs were synthesized using 200 ng of RNA, SUPERSCRIPT II RNase H$^-$ Reverse Transcriptase (Invitrogen), and random hexamers (Invitrogen). Of each first-strand reaction, 2 μl was taken as template in PCRs using cDNA Advantage Polymerase (BD Biosciences Clontech) (primer sequences are available from the authors on request). For amplification of the coding region of *CEP55*, we used 2 μl of each first-strand reaction in PCRs using cDNA Advantage Polymerase (BD Biosciences Clontech) and primers MultiRT4 (5′-GACCGTTGTCTCTTCGATCGCTTC-3′) and Multig2 (5′-GTATTCCACATGGACAAGCAGATC-3′). Amplicons were cloned and sequenced. The resulting clone pMG42 was used as starting material for the generation of EGFP fusion proteins by the GATEWAY system (see below).

Northern blot analysis

A 580-bp PCR product containing part of the *CEP55* cDNA was amplified with primers O02F (5′-GCAGTGGCTCGTGTATGATCAGC-3′) and O02R (5′-GATGCTGCACATGTTGACGGTCG-3′) and radiolabeled by random

priming with hexanucleotides (Invitrogen; Amersham Biosciences) and [α-^{32}P]-dCTP (Amersham Biosciences). A commercial human multiple tissue blot (MTN, BD Biosciences Clontech) was hybridized according to the manufacturer's instructions, washed at high stringency, and exposed to X-ray film. Positive signals were detected by autoradiography. To control for RNA integrity and loading amount, the blot was rehybridized with α-^{32}P-labeled β-actin probe as described in the protocol provided. A commercial human multiple tissue expression array (MTE, BD Biosciences Clontech) was hybridized according to the manufacturer's instructions, washed at high stringency, and exposed to X-ray film.

Antibody production

A cDNA fragment corresponding to amino acids 2–250 of CEP55 was subcloned in-frame into pGEX-3T plasmid (Amersham Pharmacia Biotech). The glutathione *S*-transferase (GST)–CEP55 fusion protein was expressed in *Escherichia coli* BL21 and purified with glutathione–agarose beads by using the Bulk and RediPack GST purification modules (Amersham Pharmacia Biotech) according to the manufacturer's instructions. Anti-CEP55 antibodies were raised by immunizing rabbits with the GST–CEP55 protein (aa 2–250) (Biogenes). The IgG fraction of this antiserum was purified (named AK40-5307) (Biogenes).

Generation of an N-terminal-tagged enhanced green fluorescent protein CEP55 fusion construct

For PCR amplification of the coding region of *CEP55*, we used pMG42 as a template and primers MultiC3F (5′-GGGGACAAGTTTGTACAAAAAAG-CAGGCTTGTCTTCCAGAAGTACCAAAG-3′) and MultiC3R (5′-GGGGACCACTTTGTACAAGAAAGCTGGGTGTTACTACTTTGAACAG-TATTCCAC-3′) for constructing an N-terminal EGFP fusion construct. Amplification was performed by using cDNA Advantage polymerase (BD Biosciences Clontech) and the PCR product was purified according to the instructions of the GATEWAY system. Cloning of the PCR product into "donor vector" pDONR207 (Invitrogen) via BP reaction yielded clone pMG47. Verified clones were used for cloning the coding region of *CEP55* into pEGFP-C3-cassetteA via LR reaction according to the manufacturer's protocol. GATEWAY-compatible plasmid pEGFP-C3-cassetteA was generated as previously described for pEGFP-N3-cassetteA [16].

Generation of the GATEWAY-compatible plasmid pMT2SM-HA-DEST and N-terminal HA- and FLAG-tagged CEP55 constructs

Plasmid pMT2SM-HA was digested with *Sma*I and *Eco*RI and purified and subsequent filling of recessed 3′ termini was performed by the Klenow fragment (Invitrogen). After alkaline phosphatase treatment and a second purification step, the plasmid was ligated to the GATEWAY Reading Frame Cassette C (RfC) of the GATEWAY Vector Conversion system (Invitrogen) according to the manufacturer's instructions. The obtained GATEWAY-compatible "destination vector," pMT2SM-HA-DEST, was propagated in *E. coli* DB3.1 (Invitrogen) to compensate for the expression of the *ccdB* gene. The plasmid was sequenced for integrity and correct orientation of the cassette. pMG47 was used for cloning the coding region of *CEP55* into vectors pMT2SM-HA-DEST and pFLAG-CMV-4-cassetteA [33] via LR reaction according to the manufacturer's protocol. All described constructs were sequenced for integrity and large and pure amounts of plasmid DNA were prepared by using a plasmid midi or maxi kit (Qiagen).

Cell culture and synchronization

CHO-K1 cells were maintained in F12-Ham's Nutrient Mixture (Invitrogen) supplemented with 10% FCS, 1% L-glutamine, and penicillin–streptomycin (Invitrogen). To obtain cells synchronized at M phase, CHO-K1 cells were grown on coverslips (analysis of fixed cells) or on LabTek chambered 4-well coverglasses (Nalge Nunc) (for videomicroscopic analysis) to 40–70% confluency and treated with 5 mM thymidine (Sigma) for 17 h to arrest the cell cycle at the S and G1–S stages. Subsequently, cells were washed and incubated at 37°C for 5 h. Cells were exposed to 0.05 μg/ml nocodazole (Sigma) for an additional 5 h to arrest cells at prometaphase. After the drug was carefully washed out from the culture, cells were incubated further in fresh medium at 37°C. For cells grown on coverslips, preextraction followed by methanol fixation was performed at different time points within a 0- to 80-min period that allowed us to observe cells at different stages of mitotic progression. Cells grown on LabTek chambers were directly analyzed by time-lapsed fluorescence videomicroscopy.

Drug treatments and microtubule regrowth assay

CHO-K1 cells were treated with either 6 μg/ml nocodazole (Sigma) or 5 μM taxol (Sigma) for 4 h and then processed immediately for immunofluorescence analysis. For the microtubule regrowth assay, microtubules were depolymerized by a 4-h treatment with 6 μg/ml nocodazole and then regrowth was induced by washing the cells three times with PBS and placing them into fresh medium (without nocodazole) at 37°C for 2 min before fixation (with 4% paraformaldehyde) and immunofluorescence analysis.

Transfection

Sterile coverslips were placed in 12- and 24-well dishes and seeded with 1.2×10^5 and 2×10^4 CHO-K1 cells, respectively. Twenty-four hours later, cells were transiently transfected with an EGFP–CEP55 or HA–CEP55 fusion construct using Lipofectamine 2000 reagent (Invitrogen) according to the manufacturer's protocol. Twelve to fifteen hours after transfection, the well coverslips were rinsed with PBS and mounted with nail enamel. To obtain CHO-K1 cells stably expressing N-terminal fused EGFP to CEP55, we transiently transfected cells, split them 1/10, and incubated the cells for a further 24 h before adding geneticin (Invitrogen) to a concentration of 1 mg/ml. After 1 week, surviving cells were pooled and grown in the presence of geneticin.

Immunoblotting

Protein lysates were separated by 10% SDS–PAGE and transferred to a nitrocellulose membrane (Amersham Pharmacia Biotech) via the semidry blotting method. The membrane was blocked with 4% low-fat milk in Tris-buffered saline and then incubated with the appropriate antibody solution. Detection of bound antibodies was carried out using a ECL detection kit (Amersham Pharmacia Biotech). Anti-CEP55 antibody was used at 1:800 dilution, HRP-conjugated anti-mouse Ig (Sigma) and HRP-conjugated anti-rabbit Ig (Sigma) were used at 1:12,000 dilution, and anti-actin antibodies (Sigma) at 1:500 dilution.

Immunofluorescence

Nontransfected cells or cells 12 to 14 h after transient transfection, which were grown on coverslips, were rinsed with PBS, pre-extracted with 0.3% Nonidet P-40 (NP-40), 1 mM $MgCl_2$, 80 mM PIPES/KOH, pH 6.8, and 5 mM EGTA in 1× PBS, and fixed with 4% paraformaldehyde or in cold methanol (−20°C) for 10 min. After being washed three times with PBS for 10 min, cells were incubated with 1% BSA, 3% goat serum, and 0.5% NP-40 in PBS for 60 min to permeabilize cells and block nonspecific antibody binding. To detect γ-tubulin, cells were stained with monoclonal anti-γ-tubulin GTU-88 (1:500 dilution; Sigma), followed by incubation with Alexa Fluor 546 goat anti-mouse IgG (4 μg/ml; Mobitec). To detect α-tubulin, cells were stained with monoclonal anti-α-tubulin DM 1A (1:1000 dilution; Sigma), followed by incubation with Alexa Fluor 546 goat anti-mouse IgG (4 μg/ml; Mobitec). For detection of endogenous CEP55, cells were stained with polyclonal rabbit serum AK40-5307 or PI-AK40-5307 (pre-immune) (both at 1:1000 dilution), followed by incubation with Alexa Fluor 488 goat anti-rabbit IgG (1:1500; Mobitec). After being washed twice with high-salt PBS (650 mM NaCl) and three times with PBS, cells on coverslips were mounted in glycerol gelatin containing 1% phenol (Sigma). Cells were examined with a Leica TCS-NT confocal microscope equipped with an Apo 40 × 1.0 oil immersion objective lens.

Fluorescence videomicroscopy

High-resolution fluorescence videomicroscopy was performed with a monochromator-based imaging system (T.I.L.L. Photonics) as described in [34], except that a triple-band filter set DAPI/FITC/TRITC F61-020 (AHF Analysentechnik) was used. The imaging system was equipped with a 37°C heating control device and a 5% CO_2 supply (Live Imaging Services). For time-lapse analysis, 13 consecutive videosequences, each consisting of 100 frames with a time distance of 264 ms, were taken. The videos were finally combined into one videofile covering 52 min.

Coimmunoprecipitation

CHO-K1 cells were cultured in 100-mm culture dishes. A total of 1.2×10^6 CHO-K1 cells were transfected with pMT2SM-HA-CEP55 (4 μg DNA) and pFLAG-CMV-4-CEP55 (4 μg DNA) or pFLAG-CMV-4-cassetteA (4 μg DNA) (negative control) using Lipofectamine 2000 Reagent (Invitrogen) according to the manufacturer's protocol. After 24 h of incubation, cells were lysed with ice-cold lysis buffer [150 mM Tris–HCl, pH 8.0; 50 mM NaCl; 1 mM EDTA; 0.5% NP-40; 1 tablet Complete Mini protein inhibitor cocktail/10 ml (Roche); 0.7 μg/ml Pepstatin] and the lysates were clarified by centrifugation at 20,000*g* for 10 min at 4°C. Supernatants were applied to 50 μl EZview Red anti-FLAG M2 Agarose (Sigma) and incubated overnight at 4°C. Subsequently, the immunoprecipitates were washed three times with washing buffer (50 mM Tris–HCl, pH 7.5; 250 mM NaCl) and subjected together with total lysates to SDS–PAGE and immunoblot analysis. Proteins were detected using HRP-conjugated murine monoclonal anti-FLAG antibody (1:4000; Sigma) or HRP-conjugated rat monoclonal anti-HA antibody clone 3F10 (1:4000; Roche).

Database searches

Database searches were performed at the NCBI BLAST Network Service using numerous databases and programs. Deduced protein sequences were searched for functional domains using RRS-BLAST, PROSITE, PFAM, PSORT II, COILS, PAIRCOIL, and MULTICOIL. For prediction of the *CEP55* 5′ cDNA sequence, the High-Throughput Sequence Annotation Server RUMMAGE was used.

Note added in proof

During revision of this article, functional characterization of CEP55 was independently described by another group (Fabbro et al., Dev. Cell 9 (2005) 477–488).

Acknowledgments

The results summarized here are part of the Ph.D. thesis of Isabel Martinez-Garay at the University of Hamburg. We thank Inka Jantke and Adrian Engel (University of Hamburg) and Sigried Riese (University of Heidelberg) for skillful technical assistance. We are grateful to Georg Rosenberger for continuous support. This work was supported by a grant from the Deutsche Forschungsgemeinschaft (GRK336). H.-H. Gerdes was supported by the Deutsche Forschungsgemeinschaft (SFB 488/B2; GE 550/3-2).

Appendix A. Supplementary data

Supplementary data associated with this article can be found in the online version at doi:10.1016/j.ygeno.2005.11.006.

References

[1] S.S. Andersen, Molecular characteristics of the centrosome, Int. Rev. Cytol. 187 (1999) 51–109.
[2] B.M. Lange, Integration of the centrosome in cell cycle control, stress response and signal transduction pathways, Curr. Opin. Cell Biol. 14 (2002) 35–43.
[3] M. Kimble, R. Kuriyama, Functional components of microtubule-organizing centers, Int. Rev. Cytol. 136 (1992) 1–50.
[4] T. Stearns, M. Winey, The cell center at 100, Cell 91 (1997) 303–309.
[5] C. Cohen, D.A. Parry, Alpha-helical coiled coils and bundles: how to design an alpha-helical protein, Proteins 7 (1990) 1–15.
[6] A. Rose, I. Meier, Scaffolds, levers, rods and springs: diverse cellular functions of long coiled-coil proteins, Cell. Mol. Life Sci. 61 (2004) 1996–2009.
[7] E.H. Hinchcliffe, F.J. Miller, M. Cham, A. Khodjakov, G. Sluder, Requirement of a centrosomal activity for cell cycle progression through G1 into S phase, Science 291 (2001) 1547–1550.
[8] A. Khodjakov, C.L. Rieder, Centrosomes enhance the fidelity of cytokinesis in vertebrates and are required for cell cycle progression, J. Cell Biol. 153 (2001) 237–242.
[9] R. Heald, R. Tournebize, A. Habermann, E. Karsenti, A. Hyman, Spindle assembly in *Xenopus* egg extracts: respective roles of centrosomes and microtubule self-organization, J. Cell Biol. 138 (1997) 615–628.
[10] B.C. Dash, W.S. El-Deiry, Cell cycle checkpoint control mechanisms that can be disrupted in cancer, Methods Mol. Biol. 280 (2004) 99–161.
[11] S. Duensing, K. Munger, Centrosome abnormalities, genomic instability and carcinogenic progression, Biochim. Biophys. Acta 1471 (2001) M81–M88.
[12] E.A. Nigg, Centrosome aberrations: cause or consequence of cancer progression? Nat. Rev. Cancer 2 (2002) 815–825.
[13] M. Piel, J. Nordberg, U. Euteneuer, M. Bornens, Centrosome-dependent exit of cytokinesis in animal cells, Science 291 (2001) 1550–1553.
[14] S. Doxsey, Re-evaluating centrosome function, Nat. Rev. Mol. Cell. Biol. 2 (2001) 688–698.
[15] J.K. Schweitzer, C. D'Souza-Schorey, Finishing the job: cytoskeletal and membrane events bring cytokinesis to an end, Exp. Cell Res. 295 (2004) 1–8.
[16] I. Martinez-Garay, et al., A new gene family (FAM9) of low-copy repeats in Xp22.3 expressed exclusively in testis: implications for recombinations in this region, Genomics 80 (2002) 259–267.
[17] M. De Brabander, et al., Microtubule dynamics during the cell cycle: the effects of taxol and nocodazole on the microtubule system of Pt K2 cells at different stages of the mitotic cycle, Int. Rev. Cytol. 101 (1986) 215–274.
[18] R. Zhang, L.J. Burke, J.E. Rasko, V. Lobanenkov, R. Renkawitz, Dynamic association of the mammalian insulator protein CTCF with centrosomes and the midbody, Exp. Cell Res. 294 (2004) 86–93.
[19] A.M. Fry, P. Meraldi, E.A. Nigg, A centrosomal function for the human Nek2 protein kinase, a member of the NIMA family of cell cycle regulators, EMBO J. 17 (1998) 470–481.
[20] T. Ohta, et al., Characterization of Cep135, a novel coiled-coil centrosomal protein involved in microtubule organization in mammalian cells, J. Cell Biol. 156 (2002) 87–99.
[21] A. Khodjakov, C.L. Rieder, The sudden recruitment of gamma-tubulin to the centrosome at the onset of mitosis and its dynamic exchange throughout the cell cycle, do not require microtubules, J Cell Biol 146 (1999) 585–596.
[22] A. Gromley, et al., A novel human protein of the maternal centriole is required for the final stages of cytokinesis and entry into S phase, J. Cell Biol. 161 (2003) 535–545.
[23] L. Herrmann, T. Dittmar, K.S. Erdmann, The protein tyrosine phosphatase PTP-BL associates with the midbody and is involved in the regulation of cytokinesis, Mol. Biol. Cell 14 (2003) 230–240.
[24] M. Eda, et al., Rho-dependent transfer of Citron-kinase to the cleavage furrow of dividing cells, J. Cell Sci. 114 (2001) 3273–3284.

[25] C. Mollinari, et al., PRC1 is a microtubule binding and bundling protein essential to maintain the mitotic spindle midzone, J. Cell Biol. 157 (2002) 1175–1186.
[26] E. Hill, M. Clarke, F.A. Barr, The Rab6-binding kinesin, Rab6-KIFL, is required for cytokinesis, EMBO J. 19 (2000) 5711–5719.
[27] H.M. Thompson, A.R. Skop, U. Euteneuer, B.J. Meyer, M.A. McNiven, The large GTPase dynamin associates with the spindle midzone and is required for cytokinesis, Curr. Biol. 12 (2002) 2111–2117.
[28] A.R. Skop, H. Liu, J. Yates III, B.J. Meyer, R. Heald, Dissection of the mammalian midbody proteome reveals conserved cytokinesis mechanisms, Science 305 (2004) 61–66.
[29] A. Errico, P. Claudiani, M. D'Addio, E.I. Rugarli, Spastin interacts with the centrosomal protein NA14, and is enriched in the spindle pole, the midbody and the distal axon, Hum. Mol. Genet. 13 (2004) 2121–2132.
[30] J.C. Kim, et al., The Bardet-Biedl protein BBS4 targets cargo to the pericentriolar region and is required for microtubule anchoring and cell cycle progression, Nat. Genet. 36 (2004) 462–470.
[31] L. Romio, et al., OFD1 is a centrosomal/basal body protein expressed during mesenchymal–epithelial transition in human nephrogenesis, J. Am. Soc. Nephrol. 15 (2004) 2556–2568.
[32] J.L. Badano, T.M. Teslovich, N. Katsanis, The centrosome in human genetic disease, Nat. Rev. Genet. 6 (2005) 194–205.
[33] G. Rosenberger, I. Jantke, A. Gal, K. Kutsche, Interaction of alphaPIX (ARHGEF6) with beta-parvin (PARVB) suggests an involvement of alphaPIX in integrin-mediated signaling, Hum. Mol. Genet. 12 (2003) 155–167.
[34] A. Rustom, et al., Analysis of fast dynamic processes in living cells: high-resolution and high-speed dual-color imaging combined with automated image analysis, BioTechniques 28 (2000) 722–728, 730.